Agora of Additive Manufacturing (2024) paper24002

Agora of Additive Manufacturing

journal homepage: http://additive-manufacturing.or.jp/

Novel snap-lock fastener using 3D printed composites

Masahiro Kubota [a], Akira Todoroki [*b], and Keisuke Iizuka [c]

[a] Graduate student at Tokyo Institute of Technology, Tokyo Institute of Technology, Tokyo, Japan

[b] Department of Mechanical Engineering, Tokyo Institute of Technology, Tokyo, Japan

[c] Department of Mechanical Engineering, Aoyama Gakuin University, Kanagawa, Japan

ABSTRACT

Snap-lock fasteners are very simple for locking two parts. However, because their configuration is complex, snap-lock fasteners are usually made of polymer materials. This implies that the material is usually weak. In this study, we propose a novel snap-lock fastener printed using a 3D printer that prints continuous fiber composites. The novel fastener designed in this study can be easily attached to and detached from fastened parts. Based on the tensile test results, continuous glass fibers were placed at the elastic hinges to strengthen the weak elastic hinges. The reinforced snap-lock specimens were tested under tensile loading. Therefore, the novel snap-lock fastener with continuous glass fiber was able to bear *1.7* times higher load than that without continuous glass fibers.

Keywords: Composites, Snap-lock, Glass fiber, Carbon fiber

1. Introduction

Recently, metallic materials have been replaced with carbon fiber-reinforced polymers (CFRP) in transportation equipment, such as aircraft and automobiles. CFRP (thermosetting CFRP), which uses thermosetting resin as the base material, has better specific strength and specific stiffness than conventional metallic materials. However, manufacturing thermosetting CFRP structures requires skilled technology or large-scale/high-cost equipment. Therefore, the application of thermosetting CFRP is limited. In 2014, Markforged Inc. in the United States announced Mark One, a new thermoplastic CFRP fabrication machine that uses a fused filament fabrication (FFF) 3D printer (1). The new 3D printers enable thermoplastic CFRP fabrication by layering thermoplastics using the FFF method while extruding and cutting continuous carbon filament composites or glass filament composites extruded from a nozzle different from that of the plastic filament. Mark One and Mark Two have already been used worldwide, and the material properties of their composites have been evaluated. Frank et al. (2) evaluated the performance of a Mark One 3D printer, obtained the tensile properties, calculated the theoretical stiffness considering the difference in fiber volume content, and compared the results with experimental values. Todoroki et al. (3) obtained the mechanical properties such as tensile strength and stiffness in the fiber, transverse, shear, and lamination directions by creating continuous carbon fiber specimens with different printing directions using Mark Two and conducting tensile tests. In addition to studies on tensile properties (2)–(6), various types of mechanical properties have already been obtained, including compressive properties (7)(8), differences depending on the printing direction in impact tests (9), fatigue properties (10), and the effect of moisture absorption on the tensile properties of plastic materials (11). This 3D printer can also arrange continuous fibers in a curved shape (12),(13), and a new fracture rule for curved continuous fiber bundles has been investigated (14). Other composite 3D printers that fabricate products with high degrees of freedom are also being developed (15),(16).

---

* Corresponding author
Email: todoroki.a.aa@m.titech.ac.jp
Received 5 June 2024; Revised 24 July 2024; Accepted 26 July 2024

Composite 3D printers enable the fabrication of parts with complex configurations. A typical structure of complex parts made of polymer materials is a snap-lock, which enables us to lock two parts easily by inserting a snap-lock into a fastener hole (17)–(22). Many researchers have attempted to make snap-locks using polymer-based 3D printers (23)–(28). Because polymers are easy to mold, they are often used for snap-locks. Unfortunately, this limits the strength of the snap-locks because the strength and stiffness of the polymer are lower than those of conventional metallic materials.

In this study, a novel snap-lock fastener was developed using 3D-printed continuous-fiber-reinforced composite materials. This fastener enabled us to lock two parts using a simple snap-in process and unlock them from the surface without any additional complex processes. Using a 3D printer capable of molding complex shapes, we devised a locking mechanism with a simple locking function that cannot be easily released without a tool. Continuous fibers are used in parts where strength is required to make the structure sufficiently strong to withstand practical use. Furthermore, the developed fastener was fabricated using Mark Two, and the joint strength was obtained using a tensile fracture test.

2. Concept of novel snap-lock fastener

Thermoplastic snap-locks can be easily fastened and removed. Snap-locks are widely used to fasten two parts to which a small load is applied. In this section, as a first trial, a snap-lock fastener using short-fiber CFRP and continuous-fiber CFRP is developed to consider its application to parts that are subjected to higher loads than resin. A MarkTwo 3D printer manufactured by Markforged was used for molding. The newly developed snap-lock fastener is shown in Figs. 1 and 2. The new snap-lock fastener consists of two parts: the snap-lock pin (Fig. 1) and key (Fig. 2). The fastener with the snap-lock pin and key integrated is shown in Fig. 3.

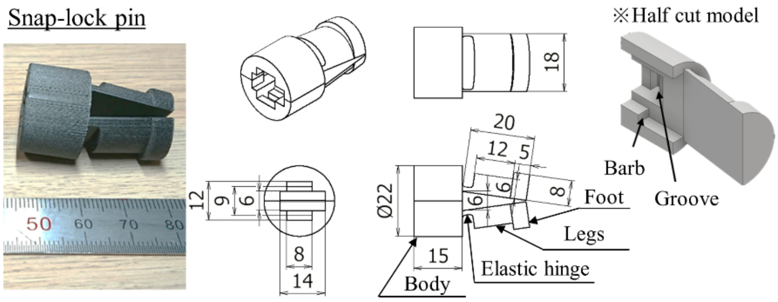

Fig. 1. Snap-lock pin.

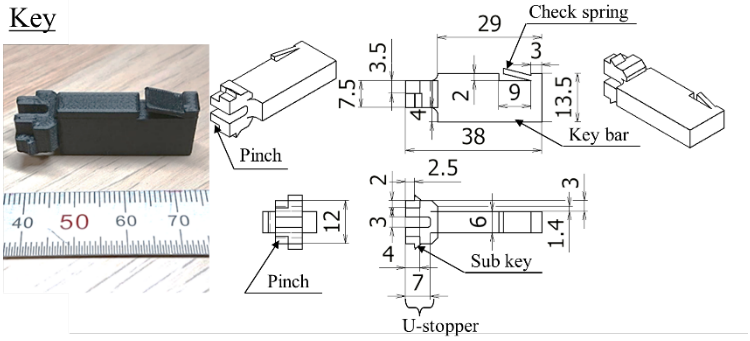

Fig. 2. Key.

Fig. 3. Assembled snap-lock pin and key.

The details of each part are explained below. The snap-lock pin has a body, legs, and feet. At the connecting parts of the body and legs, elastic hinges were designed, and the elastic hinge parts reacted to the hinges when a key was inserted between the legs. This process causes the legs to open and the opened legs lock the parts to be fastened. The grooves and barbs were designed inside the body. When the sub-key of the key is located in the groove of the snap-lock pin, the fastening process is completed.

The check spring of the key is locked at the barb of the snap-lock pin. This enables integration of the snap-lock pin and key. The key comprises a U-shaped stopper and key bar parts. When the key is inserted into the snap-lock pin, the pinch part designed on the U-shaped stopper must be grasped with a plier. The key in the snap-lock pin must be pushed by grasping the U-shaped stopper. Then, the sub-key of the key fits into the groove of the snap-lock pin, and the key is locked. Figure 4 illustrates the fastening process. The release process is shown in Fig. 5.

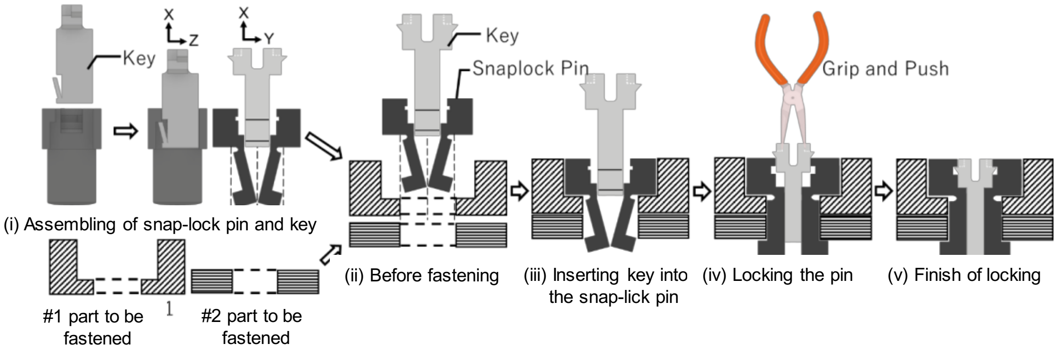

Fig. 4. Fastening process of the novel fastener.

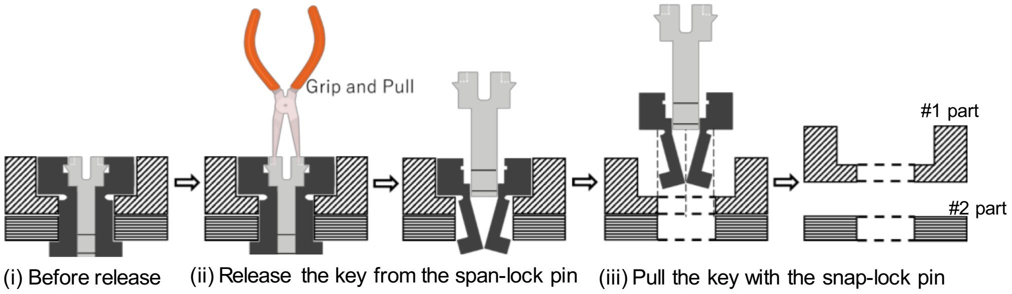

Fig. 5. Unfastening process of the novel fastener.

This snap-lock can be locked by inserting a key into the snap-lock pin. The advantages of the novel snap-lock is that it can be attached and detached only by working from one side, and is designed to prevent detachment. After fastening, a flat working surface was obtained. Moreover, one side of the fastened section was flat. The key was equipped with a check spring, and when the key was pulled out from the snap-lock pin, the check spring was caught in the grooved area, as shown in Fig. 3. When the Snap-lock fastener is removed, the Snap-lock pin is removed from the fastener by pulling on the key. Therefore, the fastener can be easily removed by accessing it from only one side (see appendix movies).

3. Tensile strength measurement of the novel snap-lock fastener

In the previous section, snap-lock function designs are described. To fasten mechanical parts, the joint strength must be higher than that of fasteners made of polymer materials. First, a short-fiber CFRP CF/PA-6 filament (Onyx®, fiber volume content of about *10* %) made by Markforged was used and molded using a MarkTwo 3D printer as a reference. Tensile tests were conducted on the molded snap-locks to confirm their strengths and weaknesses. Subsequently, we decided to reinforce the weak points with continuous fiber composites.

During the printing process, the axial direction of the cylindrical outline of the snap-lock was aligned with the in-plane direction of the 3D printer bed, and the wall-print path of the outline was placed in the axial direction. When short-fiber CFRP filaments are printed on an FFF 3D printer, the fibers are aligned in the direction of the print path. Hence, the print strength of short-fiber CFRP is the strongest in the print path direction (29). By aligning the length direction of the legs with the axial direction, the tensile strength of the legs is the strongest for short-fiber CFRP.

To obtain the joint strength, a tensile fracture test was conducted using a SHIMADZU AG-I *100* kN universal testing machine. Figure 6 shows an outline and drawing of the tensile separation jigs (upper and lower) used in the tensile fracture test, which simulate the separating force applied to the two fastened parts.

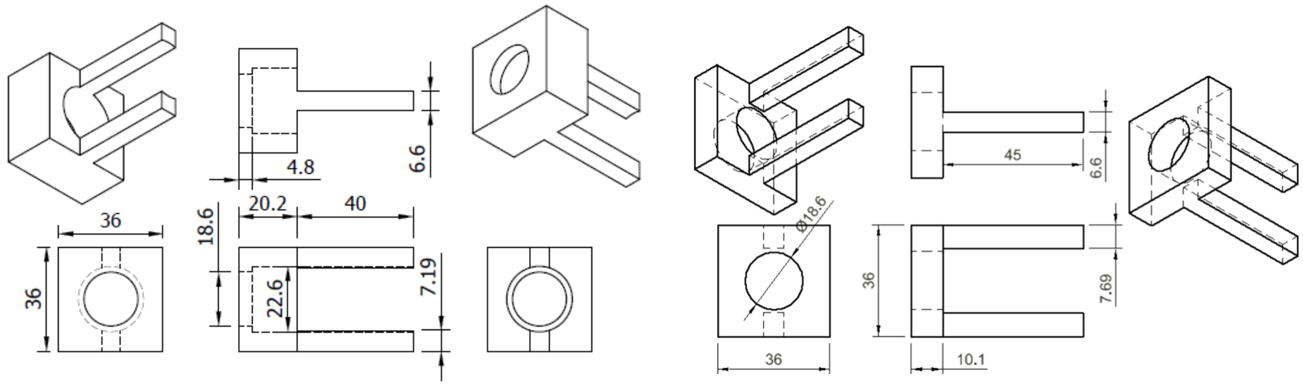

(a) Upper jig (b) Lower jig

Fig. 6. Upper and lower jigs for tensile tests of the novel snap-lock system.

After the snap-lock fastener was fastened, the upper and lower fastened members were gripped using testing machine jigs and subjected to tensile loading. Figure 7 shows the configuration of the tensile-failure test setup. The printing path of the snap-lock fastener is shown in Fig. 8. Three tests were conducted.

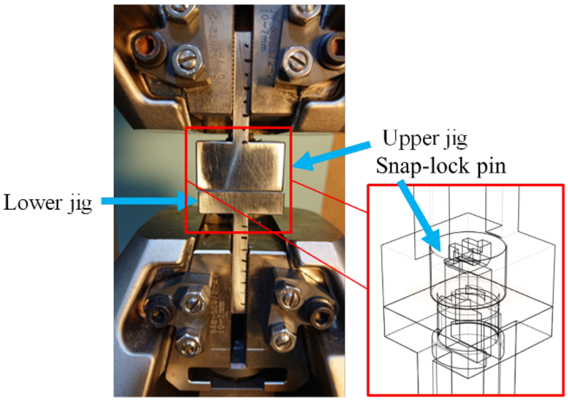

Fig. 7. Tensile fracture test setup. The snap-lock is inside the upper and lower jigs.

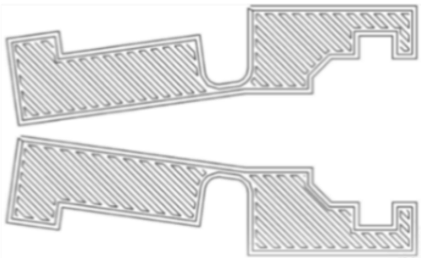

Fig. 8. In-fill pattern of the snap-lock pin with Onyx filament.

The load–displacement relationships obtained from the tensile fracture tests are shown in Fig. 9. The abscissa represents the displacement of the testing machine and the ordinate represents the tensile load. The load–displacement diagrams show that there was no significant scatter in the three tests. The average value of the load when the load dropped significantly was *2.63* kN for the three specimens.

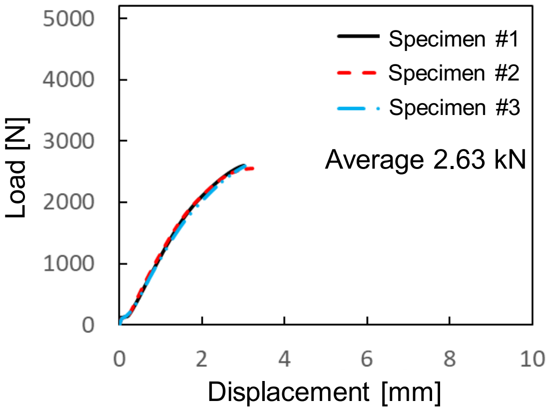

Fig. 9. Load–displacement diagram of the fastener made from Onyx with fill rate *100* %.

The specimen after fracture is shown in Fig. 10. Figure 10 shows a snap-lock pin that ruptures at the elastic hinge. This indicates that the elastic hinge should be reinforced with continuous fibers.

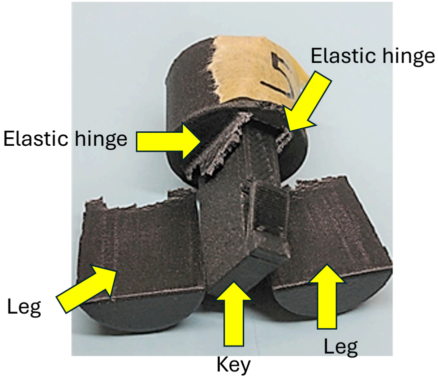

Fig. 10. Configuration of the fractured novel fastener after the tensile fracture test.

4. Strength Improvement using continuous glass fiber composites

To develop a higher-strength snap-lock fastener than that made of short CF/PA-6 fiber (Onyx), the elastic hinge nodes must be reinforced with continuous fibers. Therefore, we changed the fiber placement in the slice software to strengthen the leg portion of the snap-lock fastener with continuous glass fibers. The imbedded carbon fibers increased the stiffness and impeded the action of the hinge. Thus, a continuous glass fiber was adopted in this section.

When modeling with MarkTwo®, it is necessary to slice the modeling parameters with Eiger®, which is a cloud-based slicing software. The molding parameters that can be set are restricted by Eiger®. Continuous fibers that can be placed in the same plane are limited to one direction. Therefore, when the snap-lock pin developed in this study was sliced from a single STL data point, only one side of the elastic hinge could be strengthened, as shown in Fig. 11. This indicates that we must divide the snap-lock pins into two STL datasets: left and right. Next, we must use the slice software Eiger® for each (left and right) part separately to strengthen both elastic hinge parts. To obtain a perfectly integrated snap-lock pin, we printed two parts (left and right) simultaneously within the contact distance. We simply placed the left part (Part 1 in Fig. 12) and right part (Part 2 in Fig. 12) side by side on the print bed within the contact distance. To improve the bonding between the two parts, we added the adhesive layer STL data, which is part 3 in Fig. 12. All parts (Parts 1 to 3) were printed simultaneously. The distance between Part 1 and Part 2 was *0* mm, and Part 3 overlaps Part 1 and Part 2 by *0.7* mm each. Figure 13 shows the print paths of the Onyx®-only layer and glass-fiber reinforced layer.

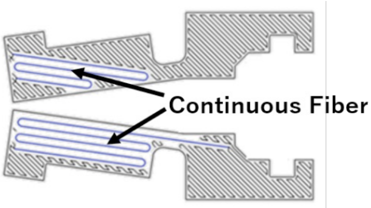

Fig. 11. Print path made with the Eiger® slice software when the snap-lock pin is sliced as an integrated part. The gray lines indicate print paths of Onyx®. Blue lines indicate continuous glass fiber paths. The slice software Eiger places continuous fiber paths in unidirectional placement or in concentric placement in a sliced plane in a part.

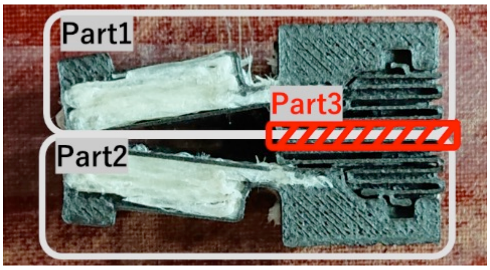

Fig. 12. Three parts are printed simultaneously. This process enables us to make an integrated snap-lock pin with reinforcement of unidirectional glass fibers in both legs. The part #3 is indispensable to make an integrated snap-lock pin.

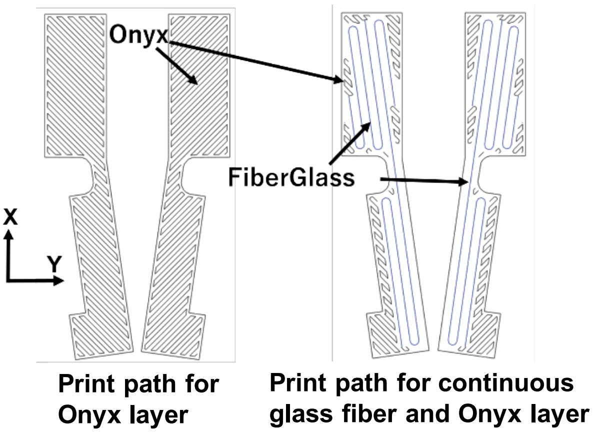

Fig. 13. 3D printed path of the fiberglass reinforced snap-lock pin.

A continuous glass-fiber-reinforced fastener was fabricated using a Mark Two 3D printer. The printed fasteners were subjected to tensile fracture tests, as described in the previous section. Three different snap-lock pin specimens were prepared with different numbers of continuous glass fiber layers: *20* (*2.0* mm), *40* (*4.0* mm), and *60* (*6.0* mm). The load–displacement diagrams for the tensile fracture test of each type of specimen are shown in Figs. 14(a)–(c). The load–displacement diagrams show that there is no significant variation in the continuous fiber-reinforced fasteners fabricated with MarkTwo®. The MarkTwo® uses the same fabrication parameters that is created by the slice software Eiger and the parameters are not open to users. The average values of the three loads when the load dropped significantly were *3.79* kN for the *20*-layer reinforced specimen, *3.97* kN for the *40*-layer reinforced specimen, and *4.49* kN for the *60*-layer reinforced specimen. Failure occurred at the foot of the snap-lock pin in all specimens. As the average maximum load of the specimens made from the short-fiber CF/PA-6 (Onyx) was only *2.63* kN, the reinforcement of continuous glass of *60* layers gives approximately *70* % increase of the maximum load without increase of difficulty of pushing the key.

A typical photograph of a specimen after fracture is shown in Fig. 15. As indicated by the arrows in the figure, the fracture occurred at the foot of the snap-lock pin. This indicates that the elastic hinge area was successfully strengthened using continuous glass fibers. The fracture load of the 60-layer glass-fiber-reinforced fastener specimen was *1.7* times higher than that of the short-fiber CF/PA-6 fastener. A higher load indicates that the continuous glass fiber reinforcement was successful at the elastic hinge.

Further strength improvements can be expected by changing the dimensions of the leg portion and modifying the leg portion to include continuous fibers. Moreover, shear strength is also important for some snap locks. These will be the focus of our future work.

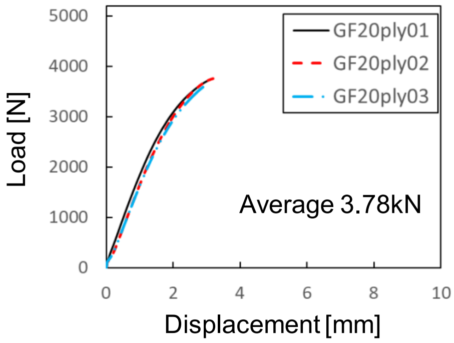

(a) 20 UD glass layers.

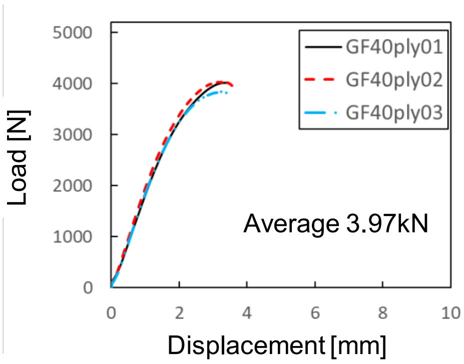

(b) 40 UD glass layers

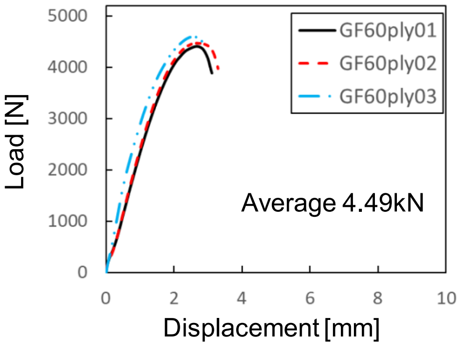

(c) 60 UD glass layers

Fig. 14. Load–displacement diagram of the snap-lock tensile tests for number of UD glass layers.

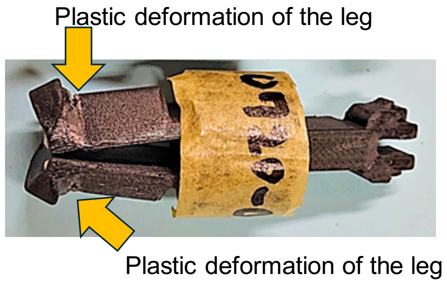

Fig. 15. Failure mode of the snap-lock after the tensile test.

5. Conclusions

In this study, we propose a novel snap-lock fastener that can be printed using a 3D printer (Mark Two). The fastener can be easily attached to and detached from the fastened parts. Based on the tensile test results, continuous glass fibers were placed at the elastic hinge parts. The reinforced snap-lock specimens were tested under tensile loading. The following results were obtained:

(1) By exploiting the characteristics of 3D printed composite materials, we developed a fastener that can be easily joined and removed from only one side.

(2) The bonding strength of the fasteners was obtained by modeling the developed fasteners with MarkTwo and conducting a tensile fracture test. We found that an onyx fastener with a *100* % fill rate could withstand loads of up to *2.63* kN.

(3) The notched portion of the snap-lock pin, which functions as an elastic hinge when the fastener is installed or removed, was reinforced with continuous glass fibers, and actual modeling and tensile fracture tests were conducted. We found that the *60*-layer reinforcement could withstand loads of up to *4.49* kN. The use of glass fibers for fiber reinforcement enabled the development of a fastener with high joint strength without losing its function as an elastic hinge.

Acknowledgments

This research was supported in part by the IHI Corporation. Ltd..

Appendix

The STL files and MPF files of the snap-lock pin and key are included. The MPF files are the coded files for printing with Mark Two produced by Markforged ©.

<Snap-lock pin STL (https://additive-manufacturing.or.jp/agora-of-additive-manufacturing/)>
<Snap-lock pin without continuous GF MPF (https://additive-manufacturing.or.jp/agora-of-additive-manufacturing/)>
<Snap-lock pin with continuous GF MPF (https://additive-manufacturing.or.jp/agora-of-additive-manufacturing/)>
<Key STL (https://additive-manufacturing.or.jp/agora-of-additive-manufacturing/)>
<Key MPF (https://additive-manufacturing.or.jp/agora-of-additive-manufacturing/)>
The fastening process video
<https://youtu.be/-mncpNK1_YU>
The unfastening process video
< https://youtu.be/4QllZXCP9bY >

References

(1) Elisabeth E., 7th Mar., (2014), https://www.machinedesign.com/3d-printing/markforged-5000-3d-printer-prints-carbon-fiber-parts (Access 2024/4/3).

(2) Van Der Klift F, Koga Y, Todoroki A, Ueda M, Hirano Y, Matsuzaki R. 3D printing of continuous carbon fiber reinforced thermos-plastic (CFRTP) tensile test specimen. Open Journal of Composite Materials. 2016;6(1):18-27.

(3) Todoroki A, Oasada T, Mizutani Y, Suzuki Y, Ueda M, Matsuzaki R, Hirano Y, Tensile property evaluations of 3D printed continuous carbon fiber reinforced thermoplastic composites. Advanced Composite Materials. 2020;29:147-162.

(4) Melenka GW, Cheung BKO, Schofield JS, Dawson MR, Carey JP, Evaluation and prediction of the tensile properties of continuous fiber-reinforced 3D printed structures. Composite Structures. 2016;153;866-875.

(5) Naranjo-Lozada J, Ahuett-Garza H, Orta-Castañón P, Verbeeten W M H, Sáiz-González D, Tensile properties and failure behavior of chopped and continuous carbon fiber composites produced by additive manufacturing. Additive Manufacturing. 2019;26;227-241.

(6) Al Abadi H, Thai HT, Paton-Cole V, Patel V I, Elastic properties of 3D printed fibre-reinforced structures. Composite Structures. 2018;193;8-18.

(7) Justo J, Távara L, García-Guzmán L, París F, Characterization of 3D printed long fibre reinforced composites. Composite Structures. 2018;185;537-548.

(8) Bin Zakaria AZ, Takahashi T, Todoroki A, Ueda M, Kink band orientation of 3D printed continuous carbon fiber composites under compressive loading. Advanced Composite Materials. 2024;33;250-268.

(9) Caminero MA, Chacón JM, García-Moreno I, Rodríguez GP, Impact damage resistance of 3D printed continuous fibre reinforced thermoplastic composites using fused deposition modelling. Composites Part B: Engineering. 2018;148;93-103.

(10) Pertuz AD, Díaz-Cardona S, González-Estrada OA, Static and fatigue behavior of continuous fibre reinforced thermoplastic composites manufactured by fused deposition modelling technique. International Journal of Fatigue. 2020;130;105275.

(11) Chabaud G, Castro M, Denoual C, Le Duigou A, Hygromechanical properties of 3D printed continuous carbon and glass fibre reinforced polyamide composite for outdoor structural applications. Additive Manufacturing. 2019;26; 94-105.

(12) Ichihara N, Ueda M, Urushiyama Y, Todoroki A, Matsuzaki R, Hirano Y, Progressive damage simulation for a 3D-printed curvilinear continuous carbon fiber-reinforced thermoplastic based on continuum damage mechanics. Advanced Composite Materials. 2020;29;459-474.

(13) Shiratori H, Todoroki A, Ueda M, Matsuzaki R, Hirano Y, Mechanism of folding a fiber bundle in the curved section of 3D printed carbon fiber reinforced plastics. Advanced Composite Materials. 2020;29;247-257.

(14) Ishii K, Todoroki A, Mizutani Y, Suzuki Y, Koga Y, Matsuzaki R, Ueda M, Hirano Y, Bending fracture rule for 3D-printed curved continuous-fiber composite. Advanced Composite Materials. 2019;28;383-395.

(15) Yamawaki M, Kouno Y, Fabrication and mechanical characterization of continuous CFRTP using 3D printer. Journal of Japanese society of composite materials. 2017;43;97-103. (in Japanese)

(16) Matsuzaki R, Ueda M, Namiki M, Jeong TK, Asahara H, Horiguchi K, Nakamura T, Todoroki A, Hirano Y, Three-dimensional printing of continuous-fiber composites by in-nozzle impregnation. Scientific Reports. 2016;6;23058.

(17) Wang Z, Torigoe Y, Hirai S, A Prestressed Soft Gripper: Design, Modeling, Fabrication, and Tests for Food Handling. IEEE Robotics and Automation Letters. 2017;2;1909-1916.

(18) Brock JM, Wright PK, Design tool for injection molded snap fits in consumer products, Journal of Manufacturing Systems. 2002;21;32-39.

(19) Sato I, Joining of plastic parts. Journal of Japan welding society. 2009;78;634-638. (in Japanese)

(20) Watanuki K, Snap-fit design considering assemblability/disassemblability and its design review using immersive virtual environment. Journal of the adhesion society of Japan. 2007;43;149-157. (in Japanese)

(21) Rusli L, Luscher A, Sommerich C, Force and tactile feedback in preloaded cantilever snap-fits under manual assembly. International Journal of Industrial Ergonomics. 2010;40;618-628.

(22) Rousseau DS, Kolberg RF, Hotra Z, Structural Analysis of Snap-Finger Performance in Automotive Connectors. SAE Transactions. 1990;99;56-62.

(23) Klahn C, Singer D, Meboldt M, Design Consideration for Additive Manufacturing: Fused Deposition Modelling. Procedia CIRP. 2016;50;264-269.

(24) Ramírez EA, Caicedo F, Hurel J, Helguero CG, Amaya JL, Methodology for design process of a snap-fit joint made by additive manufacturing. Procedia CIRP. 2019;79;113-118.

(25) Gautam R, Idapalapati S, Feih S, Printing and characterization of Kagome lattice structures by fused deposition modelling. Materials & Design. 2018;137;266-275.

(26) Liu W, Song H, Wang Z, Wang J, Huang C, Improving mechanical performance of fused deposition modeling lattice structures by a snap-fitting method. Materials & Design. 2019;181;108065.

(27) Amaya JL, Ramírez EA, Maldonado GF, Hurel J, Detailed design process and assembly considerations for snap-fit joints using additive manufacturing. Procedia CIRP. 2019;84;680-687.

(28) He B, Li H, Jin K, Shape memory polymer actuated hollow snap-fit design analysis. Materials & Design. 2013;47;539-550.

(29) Kubota M, Hayakawa K, Todoroki A, Effect of Build-up Orientations and Process Parameters on the Tensile Strength of 3D Printed Short Carbon Fiber/PA-6 Composites. Advanced Composite Materials. 2022;31;119-136.